Article:
Qiu, L., Daniell, T.J. orcid.org/0000-0003-0435-4343, Nafees, M. et al. (9 more authors) (2025) Biochar-induced strong microbial carbon limitation prompts organic carbon sequestration and plant growth in antibiotic-contaminated soil. Plant and Soil. ISSN: 0032-079X

https://doi.org/10.1007/s11104-025-07861-1

Biochar-induced strong microbial carbon limitation prompts organic carbon sequestration and plant growth in antibiotic-contaminated soil

Linlin Qiu[a], Tim J. Daniell[b], Muhammad Nafees[c], Yihao Chen[d], Shuyu Zhou[e], Weihong Wu[a], Jia Du[a], Qingwei Zhou[a], Meiqing Jin[a], Weiying Ji[f], Jiaying Ge[f], Hongyan Guo[c,g]*

[a] College of Materials and Environmental Engineering, Hangzhou Dianzi University, Hangzhou, Zhejiang, 310012, China.

[b] School of Biosciences, University of Sheffield, Sheffield S10 2TN, UK

[c] State Key Laboratory of Pollution Control and Resource Reuse, School of the Environment, Nanjing University, Nanjing, Jiangsu, 210023, China.

[d] College of Chemical Engineering, Beijing University of Chemical Technology, Beijing, 100029, China.

[e] Shangyu Branch of Shaoxing Ecological Environment Bureau, Shaoxing, Zhejiang, 312300, China.

[f] Zhejiang Provincial Cultivated Land Quality and Fertilizer Administration Station, Hangzhou, Zhejiang, 310020, China.

[g] Quanzhou Institute of Environmental Protection Industry, Nanjing University, Quanzhou, Fujian, 362000, China.

* Corresponding author. Tel.: +86-25-89680263; Fax: +86-25-89680263.

E-mail address: hyguo@nju.edu.cn (H. Guo).

Abstract

Background and aims Organic fertilization introduces considerable antibiotics into agricultural soil. Biochar has been widely proposed as a win-win strategy for enhancing soil health, achieving carbon neutrality and improving plant growth. However, the mechanisms of how biochar enhances carbon sequestration and stimulates plant development have not been fully characterized, especially in soil containing antibiotics.

Methods As such, a greenhouse experiment was conducted to investigate the microbial-driven pathways by which biochar enhances soil carbon stabilization and synergistically improves plant productivity. Amplicon sequencing was adopted to analyze soil microbial community composition and untargeted metabolomics was used to understand the molecular composition of soil microbial metabolites.

Results High-temperature woody biochar increased soil organic carbon content by almost 50%, while the dissolved organic carbon was reduced by half. This induced substantial microbial carbon limitation, decreasing microbial biomass carbon content and reducing microbial carbon metabolism capability. Sulfadiazine presence could enhance biochar-induced microbial carbon limitation and has more serious impacts on soil microbial community. 107 soil metabolites changed significantly after biochar application. Enrichment analysis indicated that biochar application potentially disturbed ABC transporters and amino acid metabolism. The increased content of compounds associated with mineral and organic ion transports might promote nutrient retention in soil, leading to greater accumulation of photosynthetic pigments and increased ryegrass growth.

Conclusions We found that biochar-induced strong microbial carbon limitation prompts organic carbon sequestration and plant growth in antibiotic-contaminated soil. Understanding the intrinsic relationship between biochar-mediated soil microbial metabolism and plant growth will facilitate the advancement of low-input, high-resilience sustainable agriculture.

Keywords: biochar, antibiotic, soil organic matter, soil microbial community, carbon sequestration

1. Introduction

Soil constitutes the most significant terrestrial organic carbon sink, containing more organic carbon than global vegetation and the atmosphere combined (Paustian et al. 2016). Thus, even a tiny loss of soil organic carbon (SOC) stocks could substantially influence atmospheric CO_2 levels, leading to further global climate warming (Paustian et al. 2016; Moinet et al. 2023). Agricultural soil generally has higher percent SOC losses and is a key SOC pool that can be influenced through wise soil management to increase carbon sequestration, and remit emissions of greenhouse gas (Sanderman et al. 2017; Guenet et al. 2021). As intensive farming and sustainable agriculture advance, however, many antibiotics are introduced into agricultural soils through organic fertilizer application (Liu et al. 2024). The continuous accumulation of antibiotics held the potential to interfere SOC stock through influencing soil microbial community and metabolism process (Qiu et al. 2021). Given agriculture's vital role in climate mitigation, prioritizing efficient soil carbon sequestration strategies that account for antibiotic impacts is essential for achieving carbon neutrality.

Biochar has been extensively advocated as a win-win strategy to achieve carbon sequestration and immobilize contaminants (Luo et al. 2023). Biochar can potentially moderate native SOC decomposition through positive, neutral, or adverse priming effects to influence carbon sequestration (Maestrini et al. 2014). The composition of biochar and SOC, nutrient availability, and microorganisms are the main drivers of controlling the direction of priming effects (Luo et al. 2023). For example, low-temperature biochar is abundant in labile organic carbon, which can stimulate soil

74 microorganisms growth and expedite the decomposition of SOC with positive priming
75 effects in the short term (Kuzyakov 2010; Ren et al. 2022). However, adverse priming
76 effects frequently arise from the suppression of soil microorganisms, whether due to
77 microbial C limitation induced by sorption-reduced labile C availability or due to direct
78 toxicity from noxious biochar substances. Significantly, biochar-induced increased
79 competition between keystone taxa can also lead to adverse priming effects enabling
80 SOC sequestration, even though biochar application typically stimulates the soil
81 microorganism biomass and diversity (Chen et al. 2019). Current studies fail to
82 reconcile these contradictory mechanisms and establish consistent conclusions
83 regarding the long-term implications of biochar application for native SOC persistence.
84 Porous structure and large specific surface area endow biochar with a substantial
85 adsorption property, effectively immobilizing antibiotics. Han et al. (2024) found that
86 biochar significantly reduced antibiotic availability in soil, concurrently reshaping soil
87 microbial community composition. In contrast, there is also some evidence that shows
88 biochar-sorbed antibiotics retain bioavailability for soil microbes (Wang et al., 2020).
89 Moreover, Qiu et al. (2025) indicated that antibiotic-induced disturbances to soil
90 microbial structure and function still exist after biochar application. Consequently,
91 reconciling biochar's dual effects on antibiotic bioavailability and microbial resilience
92 remains critical for deploying it as a reliable carbon sequestration enhancer in
93 antibiotic-polluted soils.
94 Although biochar has been demonstrated to be a strong candidate to aid an increase in
95 carbon sequestration and pollution immobilization, deep insight into the mechanisms

underlying C cycling and sequestration remains largely unexplored, especially in antibiotic-contaminated soils. In general, the core issue required to allow a comprehensive evaluation of biochar's potential and feasibility as a carbon sequestration strategy hinges on its impact on the molecular composition and speciation of indigenous organic carbon. However, soil organic carbon turnover exploration has been restricted by SOC chemical complexity and spatial heterogeneity. As a nascent technology, soil metabolomics shows potential to provide a greater understanding of carbon cycling. Untargeted soil metabolomics offers a global analysis of specific metabolites of low molecular weight (<1000 Da), allowing the identification of molecular networks and cellular pathways. Studies have confirmed that this approach elucidates key biological mechanisms in terrestrial carbon cycling (Swenson et al. 2015; Withers et al. 2020).

To sum up, biochar demonstrates promise for regulating soil carbon cycling and facilitating pollution remediation. However, existing research predominantly focuses on uncontaminated soil. A critical gap remains regarding how biochar, specifically within the stressful context of antibiotic-contaminated soil, influences core ecological processes of SOM turnover. Based on our current understanding, we hypothesis that antibiotic would influence SOM composition through affecting soil microbial community composition and function. Biochar application would induce distinct shifts in SOM composition in antibiotic-contaminated soil compared to uncontaminated controls, mediated through microbial community restructuring and functional adaptation. To test these hypotheses and address this gap, a pot experiment was

designed to: (i) investigate the mechanisms by which biochar addition alters the content and chemical composition of SOM in antibiotic-contaminated versus uncontaminated soil; (ii) elucidate biochar-driven shifts in soil bacterial community structure, diversity, and carbon-cycling functional traits under antibiotic stress; (iii) decipher the interactive mechanisms through which biochar enhances carbon sequestration efficiency and stimulates plant development in antibiotic-impacted soil systems.

2. Material and methods

2.1 Experiment design

Topsoil classified as Anthrosol was collected from a farmland in Zhejiang province, China (29°47′ N, 121°21′ E). Detailed information about the soil is shown in Table S1. A given mass of sulfadiazine (SDZ) was added to the air-dried soil to attain a final concentration of 5 mg kg^{-1}. This set concentration is comparable to the concentrations found in agricultural soil near feedlots (Ji et al., 2012), representing a relatively high field condition. The biochar employed in this investigation was synthesized through a standardized pyrolysis protocol. Air-dried sawdust underwent a slow pyrolysis process with a heating rate of 15 °C min^{-1} to a terminal temperature of 500°C, maintained for 2 hours in a muffle furnace under oxygen-limited conditions using continuous flowing N_2 as the medium gas. The biochar was mechanically ground and passed through a 2-mm mesh sieve before use. The basic physicochemical properties were displayed in Table S2 and Fig. S1 in the supplementary material. Biochar was mixed with the above two soils in a proportion of 3:100 (mass ratio). Then, 100 g soil or the mixture of soil and biochar was packed into plastic containers to yield control (CK: 0 mg kg^{-1} of SDZ),

SDZ addition (SDZ: 5 mg kg^{-1} of SDZ), biochar addition (B: control soil + 3% biochar), SDZ and biochar addition (SDZB: 5 mg kg^{-1} of SDZ + 3% biochar) treatment. The experimental design incorporated four biological replicates for each treatment.

Ryegrass seeds were disinfected using 10% H_2O_2 solution, washed three times with ddH_2O, and sprouted on autoclaved paper towels for a week. Twenty treated ryegrass seeds with similar growth were transplanted into each pot, and water was added to achieve 60% field capacity. After a 40-day incubation, ryegrass was separated from the soil, and total fresh biomass was determined. Soil samples were collected and subdivided into three discrete aliquots. One was air-dried for basic physicochemical index determination and dissolved organic matter extraction. One was collected and stored at 4 ℃ for microbial carbon metabolic activity evaluation. The remainder was stored at – 80 ℃ for soil microbial community and metabolomics analysis.

2.2 Photosynthetic pigments determination

The content of photosynthetic pigments was determined following the protocol of Lichtenthaler (1987). In brief, 0.25 g ryegrass leaf samples were weighted and mixed with 5 mL 80% acetone solution for 12 h in the dark. After centrifugation, the supernatant detects absorbance at 663 nm, 645 nm, and 470 nm using a microplate reader (Varioskan LUX, Thermo Fisher Scientific, Vantaa, Finland).

2.3 Soil organic carbon composition characterization

The Walkley–Black dichromate oxidation technique was employed to quantify the soil organic carbon (SOC) content (Nelson and Sommers 1982). Dissolved organic matter (DOM) was extracted following the protocol described by Oren and Chefetz (2012).

DOM quantity was assessed with a TOC analyzer (vario TOC, Elementar, Germany). Fluorescence excitation-emission matrix (EEM) spectroscopy was recorded to assess the composition of soil DOM using a F-7000 fluorescence spectrometer (Hitachi High Technologies, Japan). The fluorescence regional integration technique was employed to evaluate DOM composition (Chen et al. 2003).

2.4 Microbial biomass measurement, sequencing, and bioinformatics examination

The microbial biomass carbon (MBC) content was evaluated by determining the difference in dissolved organic carbon (DOC) between fumigated and unfumigated samples, as measured by a TOC/TN analyzer, with an applied efficiency factor of 0.45 (Wu et al. 1990).

Mobio DNeasy Powersoil kit (MoBio, Carlsbad, CA, USA) was used to extract microbial DNA from lyophilized soil. After quality and quantity checks, the V3 region of 16S rRNA gene was amplified using a universal primer pair of 341F/518R (Klindworth et al. 2012). The composition and procedure for the amplification mixture were delineated in a prior investigation (Li et al., 2018). After visualization and check, the PCR products were purified, quantified, and pooled for analysis. All amplicons were sequenced by an Ion-Torrent sequencing platform (Life Technologies, USA). After removing low-quality reads, the clean reads were de-noised using the DADA2 method and taxon classification in QIIME2 (v.2019.7) based on the Silva database (Hall and Beiko, 2018; Callahan et al., 2016; Quast et al. 2012).

2.5 Microbial carbon metabolic profiles

The metabolic capability of the soil microbial community was assessed using Biolog

EcoPlates (Biolog Inc., Hayward, CA, USA). Soil microbes were extracted according to the procedure provided by Chen et al. (2019). In brief, the mixture comprising fresh soil and sterile saline solution was shaken at 90 rpm for 30 min, followed by a 30-min static period. Subsequently, the diluted supernatant was incubated in Biolog EcoPlates at a temperature of 25°C in darkness for a duration of seven days. Color development reflects carbon utilization monitored by a microplate spectrophotometer (Thermo Scientific, USA) at 590 nm every 24 h.

2.6 Untargeted metabolomics measurement of soil metabolite

Metabolite extraction followed the protocol reported by the previous study (Qiu et al. 2021) and described in supplementary data S1. A non-targeted metabolomics investigation was conducted with a gas chromatograph (Agilent 7890B) coupled with a mass selective detector (Agilent 5977A) (Agilent Technologies Inc., CA, USA). Using highly pure helium gas as a carrier, the GC thermal program was 60 ℃ for 1 min, ramped to 125 ℃ at a rate of 8 ℃ min^{-1}, increased to 270 ℃ at a rate of 5 °C min^{-1}, 305 ℃ at 10 °C min^{-1} and finally held at 305 °C for 3 min. Mass data was obtained through a full scan from 50 to 500 m/z with 70 eV ionization energy.

2.7 Data and statistical analysis

Statistical comparisons were conducted using one-way analysis of variance (ANOVA) in SPSS 6.0 software (SPSS, Chicago, IL, USA) with Fisher's least significant difference tests. Changes in soil microbial community were assessed by principal coordinate analysis (PCoA, Anderson and Willis 2003), and the statistical significance was assessed by a permutational multivariate analysis of variance (PERMANOVA,

Anderson 2001). STAMP software was employed to investigate the dissimilarity in the microbial community because of biochar addition using Welch's t-test between two groups with Benjamini-Hochberg FDR correction (Parks et al. 2014). Statistical analyses of the untargeted metabolomic analyses were processed using MetaboAnalyst 4.0 (Chong et al. 2019). Sparse Partial Least Squares Discriminant Analysis (sPLS-DA) was performed in R (v.4.2.2) using the function "splsda" from the mixOmics package (v.6.22.0). The model was configured with the number of components (*ncomp*) set to 2 and the number of variables retained per component (*keepX*) fixed at 10, with repeated random resampling. Enrichment analysis was carried out based on differential metabolites caused by biochar addition were analyzed with the help of MB role 2.0 (López-Ibáñez et al. 2016).

3. Results

3.1 Impact of biochar application and SDZ presence on ryegrass growth

After 40 days of incorporation, both biochar application and SDZ presence improved the growth and development of ryegrass. The fresh biomass of ryegrass increased significantly from 3.66 (± 0.3) g in control to 5.46 (± 0.2) g in SDZ treatment, 7.68 (± 0.7) g in sole biochar treatment, and 6.62 (± 0.6) g in SDZB treatment ($P < 0.05$, Fig. 1a). In comparison to the control group, the application of biochar resulted in a significant increase ($P < 0.05$) in the root length of ryegrass, irrespective of whether the soil contained SDZ or not (Fig. 1b). Moreover, the photosynthetic pigments were significantly higher in the sole biochar treatment ($P < 0.05$, Fig. 1c). Specifically, the biochar-induced increase in chlorophyll a, chlorophyll b and carotenoids was 18.1%,

33.3% and 36.7% respectively. Single SDZ presence significantly increased the content of chlorophyll b and carotenoids, while this trend disappeared after biochar application.

3.2 Shift in soil organic carbon due to biochar application and SDZ presence

Our results demonstrated that biochar application raised SOC levels, both in the presence and absence of SDZ in the soil (Fig. 2a). The control contained 20.97 (± 1.31) g C kg^{-1} soil, the sole biochar treatment stored 37.93 (± 1.26) g C kg^{-1} soil and the SDZB treatment contained 41.07 (± 1.34) g C kg^{-1} soil, almost double that of the control. Whereas the DOM content was significantly reduced from 99.43 (± 5.56) to 55.55 (± 2.91) mg kg^{-1} by half due to sole biochar application (Fig. 2b). To extend understanding of DOM variation, we assessed differences in composition. As shown in Fig S2, visible changes occurred in DOM composition after biochar addition. Fluorescent region integral analysis demonstrated that humic acid-like substances were the predominant component of DOM in both the control (58.00%-65.92%) and SDZ treatment (47.43%-54.61%), whilst the distribution was more balanced after biochar application (Fig. 2c). Compared to the control, protein-like substance content exhibited a 1.32-fold elevation under biochar treatment. When antibiotics were introduced to the soil, the enhancement effect of biochar was further intensified, achieving a 2.5-fold increase in protein-like substance levels. Meantime, biochar caused an increase of approximately 50% in the proportion of both fulvic acid-like substances and soluble microbial byproduct-like substances. In contrast, a decline of 57.33% and 44.05% in humic-like substances was observed in biochar-treated control soil and SDZ-contaminated soil, respectively. To sum up, high-temperature woody biochar application lifted the SOC ceiling, reduced

the DOC content and promoted humic-like substance sequestration.

3.3 Biochar modifies soil bacterial composition and carbon metabolic ability in SDZ-amended and non-amended soils

Microbial biomass carbon (MBC) was significantly reduced (P <0.05) after biochar application, especially for soil with the presence of SDZ (Fig. 3a). No significant change was found in the microbial Shannon diversity index in sole biochar treatment, while it decreased significantly in SDZB treatment (Fig. 3b). A PCoA analysis showed a clear separation in the first dimension between the four treatments (Fig. 3c), and PERMANOVA confirmed a significant change in the microbial community because of biochar application ($P < 0.05$).

To get an insight into microbial community alternation, variations in microbial community composition at the taxonomic level were considered (Fig. 3d). The majority of bacterial ASVs were assigned to *Proteobacteria* (relative abundance ~ 34.4-22.8%) and *Actinobacteria* (relative abundance ~ 45.7.0-31.1%). Compared to control, *Proteobacteria* and *Patescibacteria* were enriched after biochar application ($P < 0.05$). Conversely, a pronounced decrease was detected in the relative abundance of *Actinobacteria* and *Gemmatimonadetes* ($P < 0.05$) in sole biochar application treatment. Moreover, there was a significant decrease in the relative abundance of *Chloroflexi* in SDZB treatment ($P < 0.05$). When assessing on an individual ASV basis 12 ASVs show significant differences between control and B treatment (Fig. 3e). ASVs assigned to *Bdellovibrio* (genus level, $P < 0.05$), *Fibrobacteraceae, Sphingomonadaceae* and *Rhodobacteraceae* (family level, all $P < 0.01$), OPB56 (order level, $P < 0.01$) and

272 *Gammaproteobacteria* (class level, $P < 0.01$) increased in relative abundance with
273 biochar addition. In contrast, ASVs assigned to *Acidobacteria* (phylum level, $P < 0.01$),
274 *Burkholderiaceae*, *Thermoanaerobaculaceae* and *Caulobacteraceae* (family level, all
275 $P < 0.05$) as well as *Solirubrobacterales* (order level, $P < 0.01$) significantly decreased
276 in relative abundance. In addition, SDZB treatment resulted in a statistically significant
277 alteration in the relative abundance of 7 ASVs compared to the control (Fig. 3f).
278 Specifically, ASVs assigned to *Solirubrobacterales* (order level, $P < 0.01$), *Opitutaceae*,
279 *Pedosphaeraceae,* and *Caulobacteraceae* (family level, all $P < 0.05$) decreased in
280 abundance under SDZB treatment. In contrast, ASVs assigned to *Saccharimonadales*
281 (order level, $P < 0.01$) and *Anaeromyxobacter* (genus level, $P < 0.01$) increased in
282 relative abundance under SDZB treatment.
283 The total microbial carbon metabolism capability was significantly decreased in B,
284 SDZ, and SDZB treatments (Fig. 4a, $P < 0.05$) with significant shifts in the respiration
285 of specific carbon compound classes. Carboxylic acids, amino acids, amines, and
286 polymers showed significantly reduced activity in B, SDZ, and SDZB treatments (Fig.
287 4a, $P < 0.05$). The metabolic activity of utilizing phenolic acids increased considerably
288 in B treatment, however, it decreased under SDZ and SDZB treatments (Fig. 4a, $P <$
289 0.05). In addition, sole biochar application did not induce changes in the utilization of
290 carbohydrates, while a significant decrease was found in SDZB treatment. Additionally,
291 SDZ induced a significant decline in normalized total microbial carbon metabolic
292 ability, while there was no significant change in B and SDZB treatment (Fig. 4b). The
293 normalized metabolic activity of utilizing carbohydrates increased significantly in B

and SDZB treatment. In contrast, both SDZ addition and biochar application could induced a noticeable decrease in the normalized metabolic activity of utilizing amino acids and amines (Fig. 4b, $P < 0.05$).

3.4 Variation in soil metabolites owing to biochar application and SDZ presence

A total of 262 soil metabolites were recognized through GC-QTOF-MS analysis. These soil metabolites primarily related to amines, amino acids, carbohydrates, fatty acids, and organic acids (Fig. 5). Results showed that carbohydrates were dominant, accounting for 35.5% - 53.6% in all four treatments (Fig. 5a). Moreover, an apparent decrease in the relative contribution of carbohydrates were detected after biochar application. In contrast, the rising relative content of amino acids and amines after biochar application was related to the suggested decreased microbial capability to utilize these two classes demonstrated by the Biolog EcoPlates (Fig. 4). A sparse partial least-squares discriminant analysis (sPLS-DA) indicated metabolites from a single SDZ presence treatment grouped with those from the control soil. At the same time, there was an apparent separation in metabolites from B and SDZB treatment in the first component, explaining 25.4% of the variance (Fig. 5f). Analysis of the loadings of PLS-DA suggested that adenosine (nucleosides), gondoic acid (fatty acids), glycerol (carbohydrates) and salicylaldehyde (amino acids) was the dominant compounds driving the separation.

More specifically, SDZ presence and biochar addition induced significant alternations in the content of 107 soil metabolites (Table S3, $P < 0.05$). Hierarchical cluster analysis further investigated the variation in soil metabolites. The heatmap covered the top 50

316 list of differential metabolites, shown in three clear clusters (Fig. 6). Cluster 1 mainly
317 contained amino acids, carbohydrates, and amines, which had an increased relative
318 content after biochar application. Specifically, biochar application increased the relative
319 content of L-glutamic acid (map00480, map00970, and map00910), 5,6-dihydrouracil
320 (map00410), and putrescine (map02010, map00480, and map00330). Within the largest
321 cluster (cluster 2), 20 compounds were under-represented after biochar application. It
322 mainly consisted of fatty acids, organic acids, and carbohydrates, with few amino acids.
323 The relative content of palmitic acid, palmitoleic acid, and myristic acid was
324 significantly decreased after biochar application, and these metabolites play an essential
325 role in fatty acid biosynthesis (map00061). Compounds in cluster 3 were the key factors
326 driving the differences between B and SDZB treatment, and organic acids were the
327 main constituents. Compared to a single biochar application, SDZ presence produced a
328 noteworthy reduction in the relative contents of glycolic acid (map00361), oxalic acid
329 (map00230), and 2-ketobutyric acid (map00290). Through enrichment analysis, we
330 found that these distinct compounds on the KEGG map were significantly involved in
331 ABC transporters (map02010), glutathione metabolism (map00480), and amino acids
332 metabolisms (map00410, map00330, map00250, map00290 and map00270) (Table S4,
333 Fig.7). Moreover, most of the metabolites related to mineral and organic ion transports
334 were up-regulated. In contrast, compounds involved in phosphate and amino acid
335 transporters were down-regulated in sole biochar application. Taken together, biochar
336 application potentially disturbed the transport and metabolism of amino acids, resulting
337 in a significantly elevated content in the soil.

4. Discussion

4.1 SDZ presence enhanced biochar-driven microbial carbon limitation

As the most biologically accessible component of SOC, soil DOC exhibits a rapid turnover rate and plays a crucial role in regulating soil CO_2 emissions (Chen et al., 2023). As an exogenous organic carbon source, biochar can regulate soil DOC turnover by applying additional DOC or adsorption of existing easily respirable DOC, influencing soil microbial processing through limitation. Biochar amendments are expected to increase soil DOC content because biochar usually contains a significant level of DOC, especially when produced at lower temperature (Liu et al. 2022a). Unsurprisingly it has been previously confirmed that soil DOC content significantly increased after addition of low-temperature biochar boosting soil microbial growth with associated and triggering of short-term positive priming effects (Ren et al., 2022: Chen et al., 2023).

In contrast, in this study using high temperature biochar soil DOC content was reduced approximately two-fold by addition (Fig. 2b), in line with with other studies that also found a decrease in DOC content when adding high-temperature produced biochar (Yang et al. 2022a, b). The decrease may associate with the porous structure of biochar, which may provide effective adsorption sites for soil DOC (Feng et al. 2021). High-temperature biochar usually exhibits a relatively high adsorption potential toward organic matter (Kasozi et al. 2010). Similarly, Guo et al. (2020) also indicated that high-temperature biochar caused a lowered soil DOC due to stronger carbon limitation. Moreover, Chen et al. (2022) suggested that woody biochar can cause stronger

360 microbial carbon limitation than crop residue biochar. The woody biochar produced at
361 500 ℃ used in our study possesses large surface areas (S_{BET}: 525.28±18.20 m^2/g, Table
362 S2), porous structure, and various functional groups (Fig. S1), expected to have strong
363 adsorption of organic matter.
364 More importantly, DOC content significantly decreased in SDZB treamtment compared
365 to the B treatment. The behind reason might be that antibiotic inhibited microbial
366 activity and weaken DOC decomposition, leading to temporary accumulation of DOC.
367 This excess DOC can be adsorbed by biochar and immobilized as non-extractable forms,
368 thereby decreasing measurable DOC concentrations. Additionally, antibiotic stress
369 forces soil microbes into a "maintenance metabolism" state, diverting energy to
370 resistance mechanisms instead of growth. Consequently, less DOC is converted into
371 microbial biomass, increasing the pool of DOC immobilized through biochar
372 adsorption. Our results suggested that SDZ presence can enhance biochar-induced
373 microbial carbon limitation.

374 **4.2 Strong microbial carbon limitation caused significant alternations in soil**
375 **bacterial community composition and fuction**

376 Although high-temperature biochar, such as that used in this study, offers more
377 habitable space for many soil microbes, its limited available labile carbon substrates
378 resulted in a reduced overall population size (Fig. 3a). Single biochar application
379 induced the shift in the soil microbial community composition by stimulating the
380 relative abundance of *Proteobacteria* and *Patescibacteria,* in agreement with the
381 findings reported in previous studies (Liu et al. 2022b; Lu et al. 2020; Gao et al. 2017).

Through further analysis, we found that *Gammaproteobacteria* (class level), *Sphingomonadaceae* and *Rhodobacteraceae* (family level), and *Bdellovibrio* (genus level) were the main contributors to the increased relative abundance of *Proteobacteria* (Fig. 3c). Biochar can provide shelter to *Proteobacteria* for its colonization, growth, and multiplication (Tan et al. 2022). *Rhodobacteraceae* involved in soil carbon and nitrogen cycle (Fortuna et al. 2011), and its increased relative abundance indicated a direct impact of biochar application on SOM turnover. *Burkholderiaceae* (order *Burkholderiales*) includes opportunistic pathogens and can cause severe disease (Rhodes and Schweizer 2016), and *Bdellovibrio* are versatile predatory bacteria with great potential as antimicrobial agents (Oyedara et al. 2018). The increased relative abundance of the genus *Bdellovibrio* and decreased relative abundance of the order *Burkholderiaceae* provided support for the potential capability of biochar in mitigating soil-borne pathogens. Moreover, our results displayed a significant decrease in the relative abundance of *Actinobacteria* and *Gemmatimonadetes*, as reported by previous studies (Gao et al. 2017; Li et al. 2022). *Actinobacteria* serves as a consumer of carbon-rich and recalcitrant substances, while *Gemmatimonadetes* exhibit potential as degraders of recalcitrant carbon compounds (Lehmann et al. 2011). The significant decrease in the relative abundance of these soil recalcitrant carbon-degrading microbes hold the potential to promote SOC stabilization. In addition, biochar-mediated alterations to soil properties (e.g., porosity, pH, cation exchange capacity) can also drive shifts in microbial community composition. There was a significant decrease in the relative abundance of the phylum *Acidobacteria*. It might relate to the higher pH in

biochar treatment, which is unfavorable for its growth (Table S5).

Compared to sole biochar application, MBC significantly decreased in SDZB treatment (Fig. 3a). Notably, no significant changes in Shannon diversity were observed with individual biochar or SDZ treatments, yet their co-application significantly suppressed diversity (Fig.3b). The above results indicated that SDZ enhanced biochar-induced microbial carbon limitation and resulted in more serious impacts on soil microbial community. The metabolism capability of carbohydrates, carboxylic acids, amino acids, polymers, phenolic acid and amines significantly decreased in SDZ treatment. It was in line with previous studies that showed antibiotic-mediated microbial death is a complex process entailing both primary target inhibition and subsequent metabolic alterations (Yang et al. 2019). Moreover, our results showed that decline in carbohydrate metabolism activity directly reflected carbon-limited population crashes, while reduced amino acid metabolism signaled functional shifts (Fig. 4). Enrichment analysis showed that biochar amendment perturbed amino acid metabolism, particularly affecting beta-alanine metabolism and arginine-proline metabolism pathways (Fig. 7). The possible reason might be that microorganisms prioritize maintaining core energy metabolism (such as glycolysis and the TCA cycle) and biosynthetic pathways essential for survival under carbon source limitation, while simultaneously suppressing energy-intensive and carbon-costly metabolic pathways like amino acid metabolism. In addition, biochar application has the potential to disturb glutathione metabolism (Fig. 7). The possible reason might be that soil microorganisms allocate scarce carbon resources preferentially to glutathione synthesis to maintain redox homeostasis in response to the

strong carbon limitation, soil microorganisms allocate scarce carbon resources preferentially to glutathione synthesis to maintain redox homeostasis. All the above results suggested that strong microbial carbon limitation due to DOC sorption and/or encapsulation by biochar served as the primary cause for the decline in microbial biomass and inhibited substance metabolism, indicating suppression of native SOC decomposition caused by woody biochar addition.

4.3 Biochar application promoted soil carbon sequestration and stimulated the growth of ryegrass

SOC stock is regulated by the input of exogenous carbon and mineralization (Chen et al., 2023). High-temperature woody biochar's direct input of stable organic carbon was the primary driver of elevated SOC ceilings in this study. Moreover, the biochar-induced increase in SOC storage was likely associated with the decline in SOC decomposition and the stabilization of rhizodeposits and microbial necromass (Weng et al. 2022). Strong DOC adsorption onto biochar transforms dissolved carbon into recalcitrant organo-mineral complexes, increasing SOC stability. Furthermore, woody biochar with strong adsorption capacity induced an obvious microbial carbon limitation revealed by significantly decreased DOC content, further leading to decreased microbial biomass. Combined with suppressed microbial carbon metabolism capability, biochar had the potential to retard the mineralization of native SOC. Similarly, previous studies also reported that biochar application induced negative priming effects on SOC sequestration due to DOC sorption by the biochar surface (Yang et al. 2022b; Viswanathan et al. 2023). And there are also studies that showed biochar-induced

increases in DOC can stimulate soil microbial biomass and induce short-term positive priming effects (Liu et al. 2022a, Ren et al. 2022, Chen et al. 2023). Even so, if microbes are competitive, they can decrease mineralization and promote SOC sequestration (Chen et al., 2019). Biochar can protect SOC from microbial degradation by accelerating organo-mineral formation and soil organic interfaces, thus lifting the SOC ceiling (Weng et al. 2022). Our study provided clues for the mechanism that biochar-induced strong microbial carbon limitation could help raise SOC storage through weakened mineralization.

Apart from enhancing soil carbon sequestration, biochar also has potential to promote plant growth. Biochar's inherent mineral composition (e.g., P, Ca, Mg, and Si) constitutes a readily mobilizable nutrient pool for plants and microbiota (Hou et al. 2022). Moreover, the unique structures and sorption-desorption processes endow biochar with additional utility as a slow-release fertilizer for plant growth with assertive sorption behavior enabling concentration of soil nutrients. The porous network within biochar particles and the unique interaction between nutrients and the carbon material results in slow nutrient release into the aqueous phase improving plant nutrient uptake (Wang et al. 2019). Furthermore, significant shifts occurred in the relative content of compounds associated with ABC transporter, which actively transport diverse small molecules (lipids, sugars, peptides, nutrient, etc.) across membranes in all domains of life. The increased content of compounds associated with mineral and organic ion transports indicated that biochar application might accelerate nutrient transport in soil. The above results suggested that biochar application could prompt soil carbon

sequestration and boost plant growth through nutrient supply and retention.

5. Conclusion

Our study shed light on the biological mechanisms of biochar-induced carbon sequestration and synergistic plant growth promotion. Biochar application lifted the SOC ceiling, while significantly reducing DOC content due to strong adsorption. Antibiotic presence could enhance this biochar-induced strong microbial carbon limitation, limit the growth of soil microbes and induce weaker microbial metabolism capability. Beyond its compositional nutrient supply, biochar significantly elevates soil nutrient retention via its distinct physicochemical and biological properties. The mechanistic understanding of negative priming effects due to DOC sorption and/or encapsulation by high-temperature biochar is critical to fully assess the potential of biochar application as a win-win strategy to promote plant growth and achieve carbon neutrality especially in antibiotic-contaminated soil.

Declaration of competing interest

The authors declare that they have no conflict of interest.

Author contributions

Hongyan Guo and Linlin Qiu contributed to the study conception and design. Material preparation, data collection and analysis were performed by Yihao Chen, Shuyu Zhou and Jia Du. Data management was performed by Qingwei Zhou and Meiqing Jin. The first draft of the manuscript was written by Linlin Qiu. Tim J. Daniell, Muhammad Nafees, Weihong Wu, Weiying Ji, Jiaying Ge and Hongyan Guo commented on previous versions of the manuscript. All authors have read and approved the final

manuscript.

Acknowledgments

We gratefully acknowledge the financial support of the Science and Technology Innovation Program of Jiangsu Province (grant numbers BK20220036), Science and Technology Cooperation Plan Project in "Three Rural Issues and Nine Aspects" of Zhejiang Province (grant numbers 2024SNJF066), Natural Environment Research Council (grant numbers NE/N00745X/1 and NE/S009132/1), National Natural Science Foundation of China (grant numbers 41571130061, 42173073 and 42277017).

Reference

Anderson M (2001) A new method for non-parametric multivariate analysis of variance. Austral Ecol 26: 32-46. https://doi.org/10.1111/j.1442-9993.2001.tb00081.x.

Anderson MJ, Willis TJ (2003) Canonical analysis of principal coordinates: A useful method of constrained ordination for ecology. Ecology 84: 511-525. https://doi.org/10.1890/0012-9658(2003)084[0511:CAOPCA]2.0.CO;2.

Callahan BJ, McMurdie PJ, Rosen MJ, Han AW, Johnson AJA, Holmes SP (2016) DADA2: High-resolution sample inference from Illumina amplicon data. Nat Methods 13: 581-583. https://doi.org/10.1038/NMETH.3869.

Chen LJ, Jiang YJ, Liang C, Luo Y, Xu QS, Han C, Zhao QG, Sun B (2019) Competitive interaction with keystone taxa induced negative priming under biochar amendments. Microbiome 7: 77. https://doi.org/10.1186/s40168-019-0693-7.

Chen W, Westerhoff P, Leenheer JA, Booksh K (2003) Fluorescence excitation-emission matrix regional integration to quantify spectra for dissolved organic

514 matter. Environ Sci Technol 37: 5701-5710. https://doi.org/10.1021/es034354c.
515 Chen Y, Du Z, Weng ZH, Sun K, Zhang Y, Liu Q, Yang Y, Li Y, Wang Z, Luo Y, Gao B,
516 Chen B, Pan Z, Van Zwieten L (2023) Formation of soil organic carbon pool is
517 regulated by the structure of dissolved organic matter and microbial carbon pump
518 efficacy: A decadal study comparing different carbon management strategies.
519 Global Change Biol 29: 5445-5459. https://doi.org/10.1111/gcb.16865.
520 Chen Z, Jin P, Wang H, Hu T, Lin X, Xie Z (2022) Ecoenzymatic stoichiometry reveals
521 stronger microbial carbon and nitrogen limitation in biochar amendment soils: A
522 meta-analysis. Sci Total Environ 838: 156532.
523 https://doi.org/10.1016/j.scitotenv.2022.156532.
524 Chong J, Wishart DS, Xia J (2019) Using MetaboAnalyst 4.0 for comprehensive and
525 integrative metabolomics data analysis. Curr Protoc Bioinf 68: e86.
526 https://doi.org/10.1002/cpbi.86.
527 Feng Z, Fan Z, Song H, Li K, Cheng F (2021) Biochar induced changes of soil dissolved
528 organic matter: The release and adsorption of dissolved organic matter by biochar
529 and soil. Sci Total Environ 783: 147091.
530 https://doi.org/10.1016/j.scitotenv.2021.147091.
531 Fortuna, A.M., Marsh, T.L., Honeycutt, C.W., Halteman, W.A., 2011. Use of primer
532 selection and restriction enzymes to assess bacterial community diversity in an
533 agricultural soil used for potato production via terminal restriction fragment length
534 polymorphism. Appl Microbiol Biotechnol 91: 1193-1202.
535 https://doi.org/10.1007/s00253-011-3363-7.

536 Gao L, Wang R, Shen GM, Zhang JX, Meng GX, Zhang JG (2017) Effects of biochar
537 on nutrients and the microbial community structure of tobacco-planting soils. J
538 Soil Sci Plant Nutr 17: 884-896. https://doi.org/10.4067/S0718-
539 95162017000400004.
540 Guenet B, Gabrielle B, Chenu C, Arrouays D, Balesdent JM, Bernoux M, Bruni E,
541 Caliman JP, Cardinael R, Chen SC, Ciais P, Desbois D, Fouche J, Frank S, Henault
542 C, Lugato E, Naipal V, Nesme T, Obersteiner M, Pellerin S, Powlson DS, Rasse
543 DP, Rees F, Soussana JF, Su Y, Tian HQ, Valin H, Zhou F (2021) Can N_2O
544 emissions offset the benefits from soil organic carbon storage? Global Change Biol
545 27: 237-256. https://doi.org/10.1111/gcb.15342.
546 Guo KY, Zhao YZ, Liu Y, Chen JH, Wu QF, Ruan YF, Li SH, Shi J, Zhao L, Sun X,
547 Liang CF, Xu QF, Qin H (2020) Pyrolysis temperature of biochar affects
548 ecoenzymatic stoichiometry and microbial nutrient-use efficiency in a bamboo
549 forest soil. Geoderma 363: 114162.
550 https://doi.org/10.1016/j.geoderma.2019.114162.
551 Hall M, Beiko RG (2018) 16S rRNA gene analysis with QIIME2. Methods Mol Biol
552 1849: 113-129. https://doi.org/10.1007/978-1-4939-8728-3_8.
553 Han W, Zhang M, Zhao Y, Chen W, Sha H, Wang L, Diao Y, Tan Y, Zhang Y (2024)
554 Tetracycline removal from soil by phosphate-modified biochar: performance and
555 bacterial community evolution. Sci Total Environ 912: 168744.
556 https://doi.org/10.1016/j.scitotenv.2023.168744.
557 Hou J, Pugazhendhi A, Sindhu R, Vinayak V, Thanh NC, Brindhadevi K, Lan Chi NT,

558 Yuan D (2022) An assessment of biochar as a potential amendment to enhance
559 plant nutrient uptake. Environ Res 214: 113909.
560 https://doi.org/10.1016/j.envres.2022.113909.
561 Ji X, Shen Q, Liu F, Ma J, Xu G, Wang Y, Wu M (2012) Antibiotic resistance gene
562 abundances associated with antibiotics and heavy metals in animal manures and
563 agricultural soils adjacent to feedlots in Shanghai; China. J Hazard Mater 235–236:
564 178–185. https://doi.org/10.1016/j.jhazmat.2012.07.040.
565 Kasozi GN, Zimmerman AR, Nkedi-Kizza P, Gao B (2010) Catechol and humic acid
566 sorption onto a range of laboratory-produced black carbons (biochars). Environ
567 Sci Technol 44: 6189-6195. https://doi.org/10.1021/es1014423.
568 Klindworth A, Pruesse E, Schweer T, Peplies J, Quast C, Horn M, Glöckner FO (2012)
569 Evaluation of general 16S ribosomal RNA gene PCR primers for classical and
570 next-generation sequencing-based diversity studies. Nucleic Acids Res 41: e1.
571 https://doi.org/10.1093/nar/gks808.
572 Kuzyakov Y (2010) Priming effects: Interactions between living and dead organic
573 matter. Soil Biol Biochem 42: 1363-1371.
574 https://doi.org/10.1016/j.soilbio.2010.04.003.
575 Lehmann J, Rillig MC, Thies J, Masiello CA, Hockaday WC, Crowley D (2010)
576 Biochar effects on soil biota - A review. Soil Biol Biochem 42: 1812-1836.
577 https://doi.org/10.1016/j.soilbio.2010.04.003.
578 Li F, Peng Y, Fang W, Altermatt F, Xie Y, Yang J, Zhang X (2018) Application of
579 environmental DNA metabarcoding for predicting anthropogenic pollution in

rivers. Environ Sci Technol 52: 11708-11719. https://doi.org/10.1021/acs.est.8b03869.

Li H, Xia Y, Zhang G, Zheng G, Fan M, Zhao H (2022) Effects of straw and straw-derived biochar on bacterial diversity in soda saline-alkaline paddy soil. Ann Microbiol 72: 15. https://doi.org/10.1186/s13213-022-01673-9.

Lichtenthaler HK (1987) Chlorophylls and carotenoids. Pigments of photosynthetic membranes. Methods Enzymol 148: 350-382. https://doi.org/10.1016/0076-6879(87)48036-1.

Liu H, Zhao B, Zhang X, Li L, Zhao Y, Li Y, Duan K (2022a) Investigating biochar-derived dissolved organic carbon (DOC) components extracted using a sequential extraction protocol. Materials 15. https://doi.org/10.3390/ma15113865.

Liu M, Zhu J, Yang X, Fu Q, Hu H, Huang Q (2022b) Biochar produced from the straw of common crops simultaneously stabilizes soil organic matter and heavy metals. Sci Total Environ 828: 154494. https://doi.org/10.1016/j.scitotenv.2022.154494.

Liu ZT, Ma RA, Zhu D, Konstantinidis KT, Zhu YG, Zhang SY (2024) Organic fertilization co-selects genetically linked antibiotic and metal(loid) resistance genes in global soil microbiome. Nat Commun 15(1): 5168. https://doi.org/10.1038/s41467-024-49165-5.

López-Ibáñez J, Pazos F, Chagoyen M (2016) MBROLE 2.0—functional enrichment of chemical compounds. Nucleic Acids Res 44: W201-W204. https://doi.org/10.1093/nar/gkw253.

Lu H, Yan M, Wong MH, Mo WY, Wang Y, Chen XW, Wang JJ (2020) Effects of

602 biochar on soil microbial community and functional genes of a landfill cover three
603 years after ecological restoration. Sci Total Environ 717: 137133.
604 https://doi.org/10.1016/j.scitotenv.2020.137133.
605 Luo L, Wang J, Lv J, Liu Z, Sun T, Yang Y, Zhu YG (2023) Carbon sequestration
606 strategies in soil using biochar: Advances, challenges, and opportunities. Environ
607 Sci Technol 57: 11357-11372. https://doi.org/10.1021/acs.est.3c02620.
608 Maestrini B, Herrmann AM, Nannipieri P, Schmidt MWI, Abiven S (2014) Ryegrass-
609 derived pyrogenic organic matter changes organic carbon and nitrogen
610 mineralization in a temperate forest soil. Soil Biol Biochem 69: 291-301.
611 https://doi.org/10.1016/j.soilbio.2013.11.013.
612 Moinet G, Hijbeek R, Vuuren D, Giller K (2023) Carbon for soils, not soils for carbon.
613 Global Change Biol 29: 2384-2398. https://doi.org/10.1111/gcb.16570.
614 Nelson DW, Sommers LE (1982) Total carbon, organic carbon, and organic matter. In:
615 Page AL, Miller RH, Keeney DR (eds.) Methods of Soil Analysis, Part 2, Chemical
616 and Microbiologiacl Properties, 2nd edn. American Society of Agronomy, Inc,
617 Madison, pp. 539-579.
618 Oren A, Chefetz B (2012) Sorptive and desorptive fractionation of dissolved organic
619 matter by mineral soil matrices. J Environ Qual 41: 526-533.
620 https://doi.org/10.2134/jeq2011.0362.
621 Oyedara OO, Segura-Cabrera A, Guo X, Elufisan TO, Cantú González RA, Rodríguez
622 Pérez MA (2018) Whole-genome sequencing and comparative genome analysis
623 provided insight into the predatory features and genetic diversity of two

624 *Bdellovibrio* species isolated from soil. Int J Genomics 2018: 9402073.
625 https://doi.org/10.1155/2018/9402073.
626 Parks D, Tyson G, Philip H, Beiko R (2014) STAMP: Statistical analysis of taxonomic
627 and functional profiles. Bioinformatics 30: 3123-3124.
628 https://doi.org/10.1093/bioinformatics/btu494.
629 Paustian K, Lehmann J, Ogle S, Reay D, Robertson GP, Smith P (2016) Climate-smart
630 soils. Nature 532: 49-57. https://doi.org/10.1038/nature17174.
631 Qiu L, Daniell TJ, Banwart SA, Nafees M, Wu J, Du W, Yin Y, Guo H (2021) Insights
632 into the mechanism of the interference of sulfadiazine on soil microbial
633 community and function. J Hazard Mater 419: 126388.
634 https://doi.org/10.1016/j.jhazmat.2021.126388.
635 Qiu L, Niu L, Nafees M, Zhou S, Wu W, Du J, Zhou Q, Jin M, Guo H (2025)
636 Mechanisms for sulfadiazine effective mitigation in biochar-amended soil: From
637 antibiotic resistance to soil microbial community composition and function. J
638 Environ Manage 386: 125702. https://doi.org/10.1016/j.jenvman.2025.125702.
639 Quast C, Pruesse E, Yilmaz P, Gerken J, Schweer T, Yarza P, Peplies J, Glöckner FO
640 (2012) The SILVA ribosomal RNA gene database project: improved data
641 processing and web-based tools. Nucleic Acids Res 41: D590-D596.
642 https://doi.org/10.1093/nar/gks1219.
643 Ren CJ, Mo F, Zhou ZH, Bastida F, Delgado-Baquerizo M, Wang JY, Zhang XY, Luo
644 YQ, Griffis TJ, Han XH, Wei GH, Wang J, Zhong ZK, Feng YZ, Ren GX, Wang
645 XJ, Yu KL, Zhao FZ, Yang GH, Yuan FH (2022) The global biogeography of soil

646 priming effect intensity. Global Ecol Biogeogr 31: 1679-1687.
647 https://doi.org/10.1111/geb.13524.
648 Rhodes KA, Schweizer HP (2016) Antibiotic resistance in *Burkholderia* species. Drug
649 Resistance Updates 28: 82-90. https://doi.org/10.1016/j.drup.2016.07.003.
650 Sanderman J, Hengl T, Fiske GJ (2017) Soil carbon debt of 12,000 years of human land
651 use. Proc Natl Acad Sci U.S.A. 114: 9575-9580.
652 https://doi.org/10.1073/pnas.1706103114.
653 Swenson TL, Jenkins S, Bowen BP, Northen TR (2015) Untargeted soil metabolomics
654 methods for analysis of extractable organic matter. Soil Biol Biochem 80: 189–
655 198. https://doi.org/10.1016/j.soilbio.2014.10.007.
656 Tan S, Narayanan M, Thu Huong DT, Ito N, Unpaprom Y, Pugazhendhi A, Lan Chi NT,
657 Liu J (2022) A perspective on the interaction between biochar and soil microbes:
658 A way to regain soil eminence. Environ Res 214: 113832.
659 https://doi.org/10.1016/j.envres.2022.113832.
660 Viswanathan SP, Njazhakunnathu GV, Neelamury SP, Padmakumar B, Ambatt TP
661 (2023) Invasive Wetland Weeds Derived Biochar Properties Affecting Soil Carbon
662 Dynamics of South Indian Tropical Ultisol. Environ Manage 72: 343 – 362.
663 https://doi.org/10.1007/s00267-023-01791-3.
664 Wang B, Zhang Y, Zhu D, Li H (2020) Assessment of bioavailability of biochar- sorbed
665 tetracycline to *Escherichia coli* for activation of antibiotic resistance genes.
666 Environ Sci Technol 54 (20): 12920–12928. https://doi.org/10.1021/acs.
667 est.9b07963.

668 Wang Y, Villamil MB, Davidson PC, Akdeniz N (2019) A quantitative understanding
669 of the role of co-composted biochar in plant growth using meta-analysis. Sci Total
670 Environ 685: 741-752. https://doi.org/10.1016/j.scitotenv.2019.06.244.
671 Weng ZH, Van Zwieten L, Tavakkoli E, Rose MT, Singh BP, Joseph S, Macdonald LM,
672 Kimber S, Morris S, Rose TJ, Archanjo BS, Tang C, Franks AE, Diao H,
673 Schweizer S, Tobin MJ, Klein AR, Vongsvivut J, Chang SLY, Kopittke PM, Cowie
674 A (2022) Microspectroscopic visualization of how biochar lifts the soil organic
675 carbon ceiling. Nat Commun 13: 5177. https://doi.org/10.1038/s41467-022-
676 32819-7.
677 Withers E, Hill PW, Chadwick DR, Jones DL (2020) Use of untargeted metabolomics
678 for assessing soil quality and microbial function. Soil Biol Biochem 143: 107758.
679 https://doi.org/10.1016/j.soilbio.2020.107758.
680 Wu J, Joergensen RG, Pommerening B, Chaussod R, Brookes PC (1990) Measurement
681 of soil microbial biomass C by fumigation-extraction—an automated procedure.
682 Soil Biol Biochem 22: 1167-1169. https://doi.org/10.1016/0038-0717(90)90046-
683 3.
684 Yang JH, Wright SN, Hamblin M, McCloskey D, Alcantar MA, Schrübbers L, Lopatkin
685 AJ, Satish S, Nili A, Palsson BO, Walker GC, Collins JJ (2019) A white-box
686 machine learning approach for revealing antibiotic mechanisms of action. Cell 177
687 (6): 1649–1661. https://doi.org/10.1016/j.cell.2019.04.016.
688 Yang Y, Sun K, Han L, Chen Y, Liu J, Xing B (2022a) Biochar stability and impact on
689 soil organic carbon mineralization depend on biochar processing, aging and soil

clay content. Soil Biol Biochem 169: 108657. https://doi.org/10.1016/j.soilbio.2022.108657.

Yang Y, Sun K, Liu J, Chen Y, Han L (2022b) Changes in soil properties and CO_2 emissions after biochar addition: Role of pyrolysis temperature and aging. Sci Total Environ 839: 156333. https://doi.org/10.1016/j.scitotenv.2022.156333.

Figure Captions

Fig. 1. Effects of SDZ presence and biochar application on ryegrass growth. (a) biomass of ryegrass, (b) root length of ryegrass, and (c) photosynthetic pigments of ryegrass leaves. Error bars are standard deviations of the mean of four independently prepared samples. Different letters over bars denote significant differences ($P < 0.05$).

Fig. 2. Changes in soil organic carbon due to SDZ presence and biochar application. (a) the content of SOC and (b) DOC, (c) fluorescence region integral results indicate DOC compositions of soil.

Fig. 3. Variations in bacterial community on account of SDZ presence and biochar application. (a) microbial biomass estimated by microbial biomass carbon, (b) alpha diversity estimated by Shannon index, (c) PCoA plot of bacterial community composition based on Bray-Curtis metric distance, (d) bar plots of bacterial community composition at class taxonomic levels, and extended error bar plot of distinct genera between (e) CK and B treatment and (f) CK and SDZB treatment based on Welch's t-test with Benjamini-Hochberg FDR produces at p-value < 0.05.

Fig. 4. Changes in soil (a) microbial carbon metabolism capability estimated by the average well color development (AWCD) and (b) normalized microbial carbon

712 metabolism capability estimated by the value of AWCD relative to MBC due to SDZ
713 presence and biochar application.
714 Fig. 5. Changes in soil metabolites after biochar application revealed by untargeted
715 metabolomics. Bar plots of the relative content of compounds with different
716 classification, (a) carbohydrates, (b) amines, (c) amino acids, (d) organic acids, (e) fatty
717 acids, and (f) PCA plot of soil metabolites composition based on Bray-Curtis metric
718 distance.
719 Fig. 6. Cluster heatmap of normalized peak areas for top 50 soil metabolites which were
720 significantly changed after biochar application. Metabolite row groups were colored by
721 the classification they belong to. The color of metabolite name indicated the
722 classification of the involved pathway. The pink indicated carbohydrate metabolism,
723 the orange indicated amino acid metabolism, the purple indicated lipid metabolism and
724 the blue indicated nucleotide metabolism.
725 Fig.7. The potentially perturbed biological pathways in response to SDZ presence and
726 biochar application which was drawn based on KEGG database. (a) ABC transporters,
727 (b) beta-alanine metabolism, (c) Glutathione metabolism, (d) Arginine and proline
728 metabolism. The color of soil metabolites indicated that the relative content increased
729 (orange) or decreased (green) owing to biochar application with the absence and
730 presence of SDZ in soil.

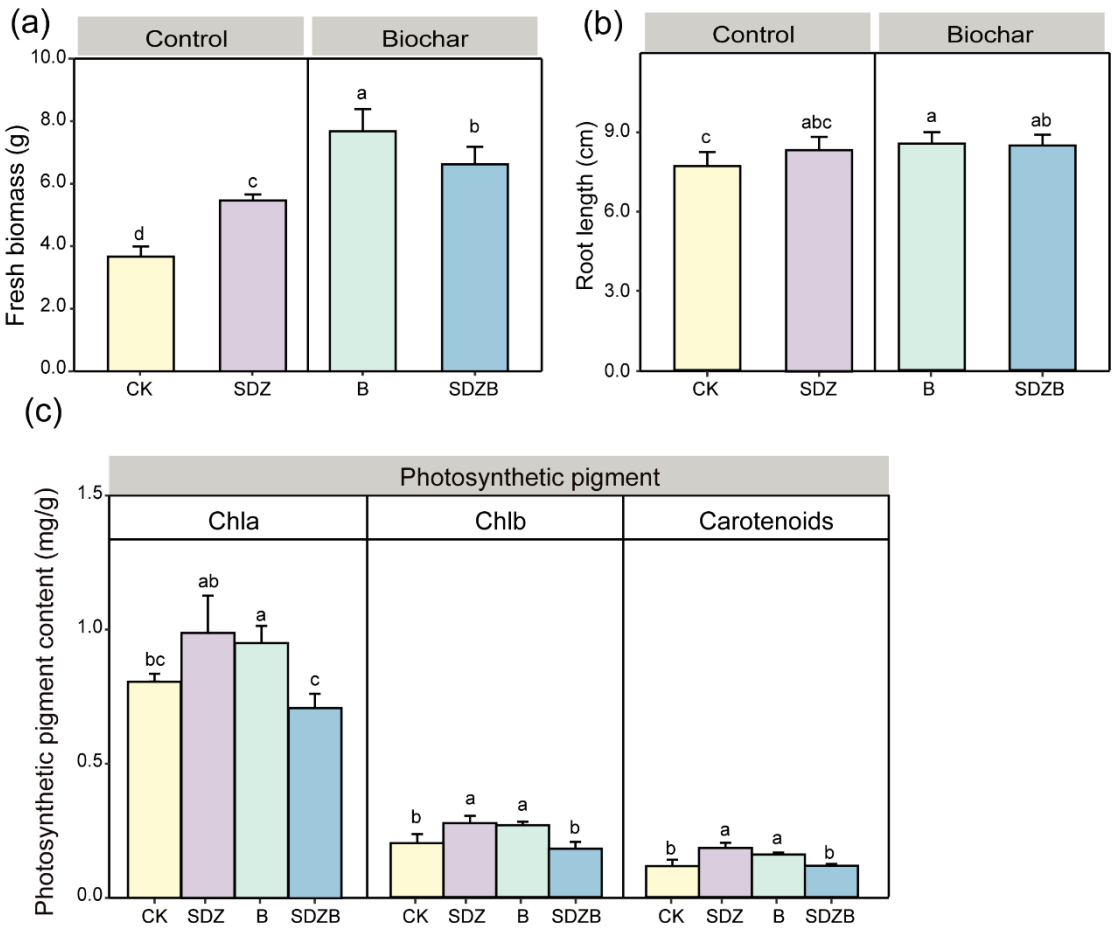
(a)
Control
Biochar
Fresh biomass (g)
10.0
8.0
6.0
4.0
2.0
0.0
d
c
a
b
CK
SDZ
B
SDZB
(b)
Control
Biochar
Root length (cm)
9.0
6.0
3.0
0.0
c
abc
a
ab
CK
SDZ
B
SDZB
(c)
Photosynthetic pigment
Chla
Chlb
Carotenoids
Photosynthetic pigment content (mg/g)
1.5
1.0
0.5
0.0
bc
ab
a
c
b
a
a
b
b
a
a
b
CK
SDZ
B
SDZB

Fig. 1

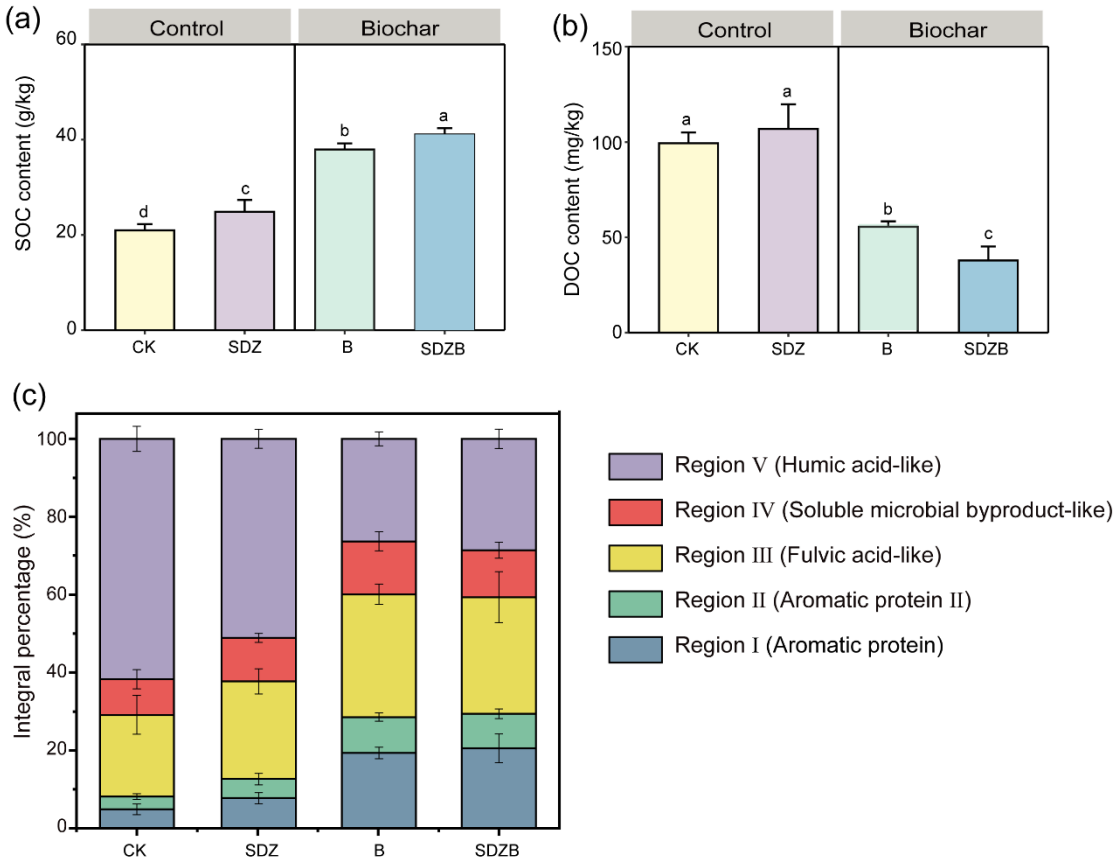
(a)
Control
Biochar
SOC content (g/kg)
60
40
20
0
d
c
b
a
CK
SDZ
B
SDZB
(b)
Control
Biochar
DOC content (mg/kg)
150
100
50
0
a
a
b
c
CK
SDZ
B
SDZB
(c)
Integral percentage (%)
100
80
60
40
20
0
CK
SDZ
B
SDZB
Region V (Humic acid-like)
Region IV (Soluble microbial byproduct-like)
Region III (Fulvic acid-like)
Region II (Aromatic protein II)
Region I (Aromatic protein)

Fig. 2

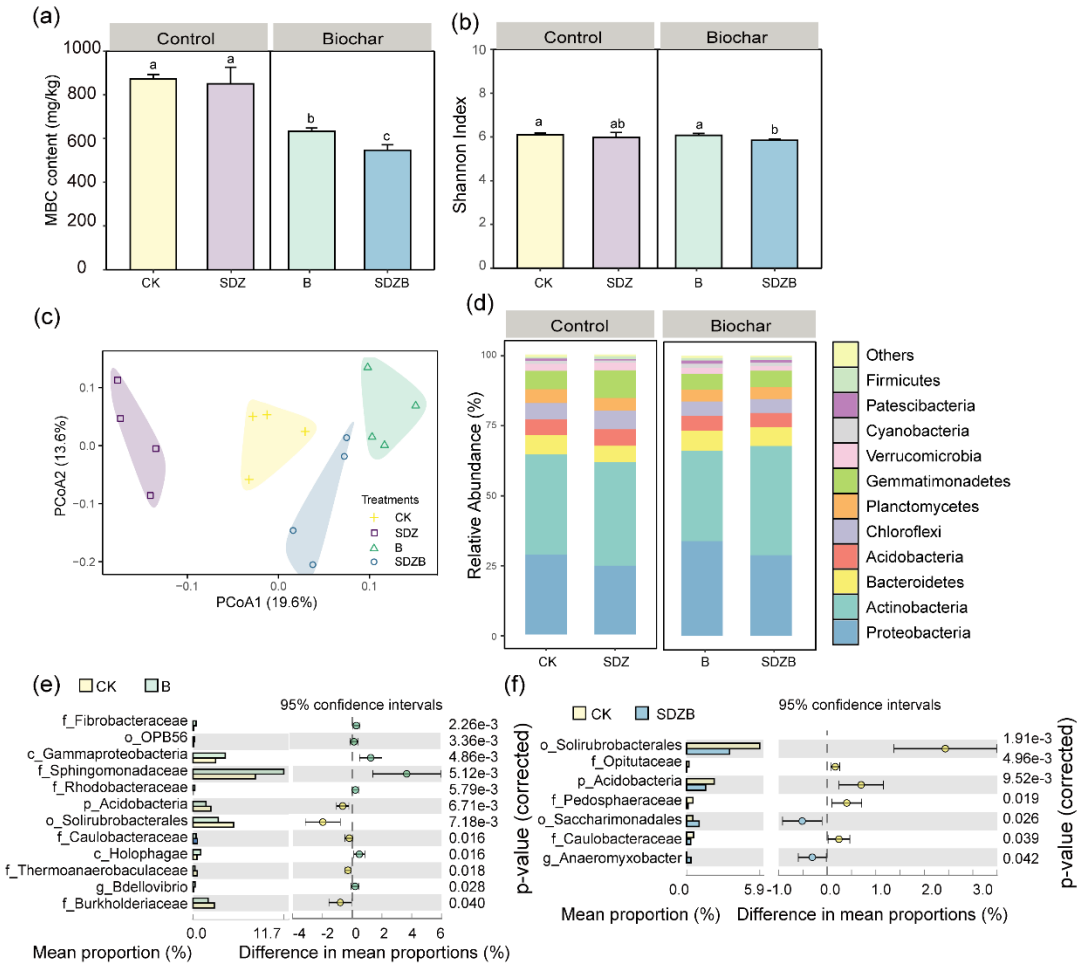
(a)
Control
Biochar
MBC content (mg/kg)
CK
SDZ
B
SDZB
(b)
Shannon Index
(c)
PCoA2 (13.6%)
PCoA1 (19.6%)
Treatments
(d)
Relative Abundance (%)
Others
Firmicutes
Patescibacteria
Cyanobacteria
Verrucomicrobia
Gemmatimonadetes
Planctomycetes
Chloroflexi
Acidobacteria
Bacteroidetes
Actinobacteria
Proteobacteria
(e)
95% confidence intervals
f_Fibrobacteraceae
o_OPB56
c_Gammaproteobacteria
f_Sphingomonadaceae
f_Rhodobacteraceae
p_Acidobacteria
o_Solirubrobacterales
f_Caulobacteraceae
c_Holophagae
f_Thermoanaerobaculaceae
g_Bdellovibrio
f_Burkholderiaceae
Mean proportion (%)
Difference in mean proportions (%)
(f)
o_Solirubrobacterales
f_Opitutaceae
p_Acidobacteria
f_Pedosphaeraceae
o_Saccharimonadales
f_Caulobacteraceae
g_Anaeromyxobacter
p-value (corrected)

Fig. 3

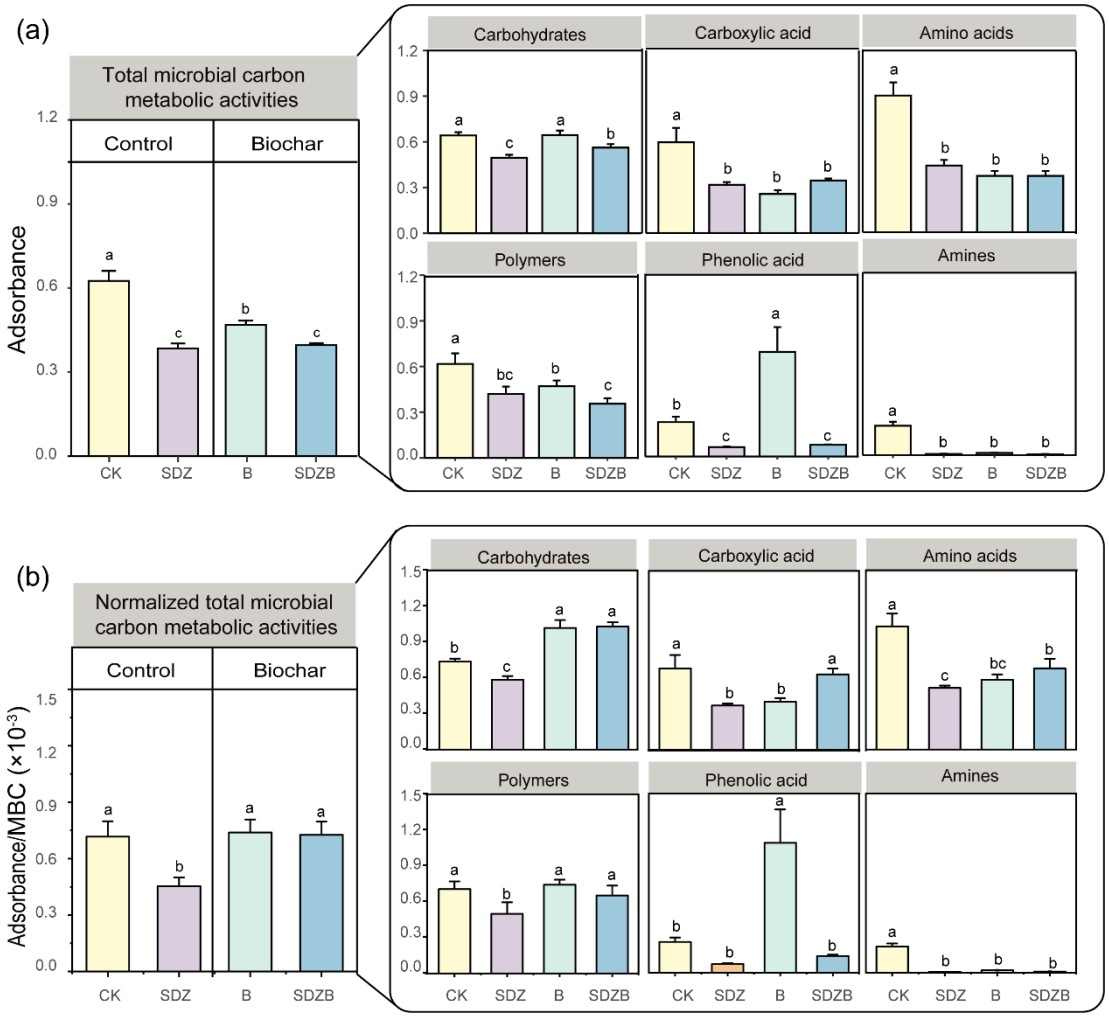
(a)
Total microbial carbon metabolic activities
Control
Biochar
Adsorbance
CK
SDZ
B
SDZB
Carbohydrates
Carboxylic acid
Amino acids
Polymers
Phenolic acid
Amines
(b)
Normalized total microbial carbon metabolic activities
Adsorbance/MBC (×10-3)

Fig. 4

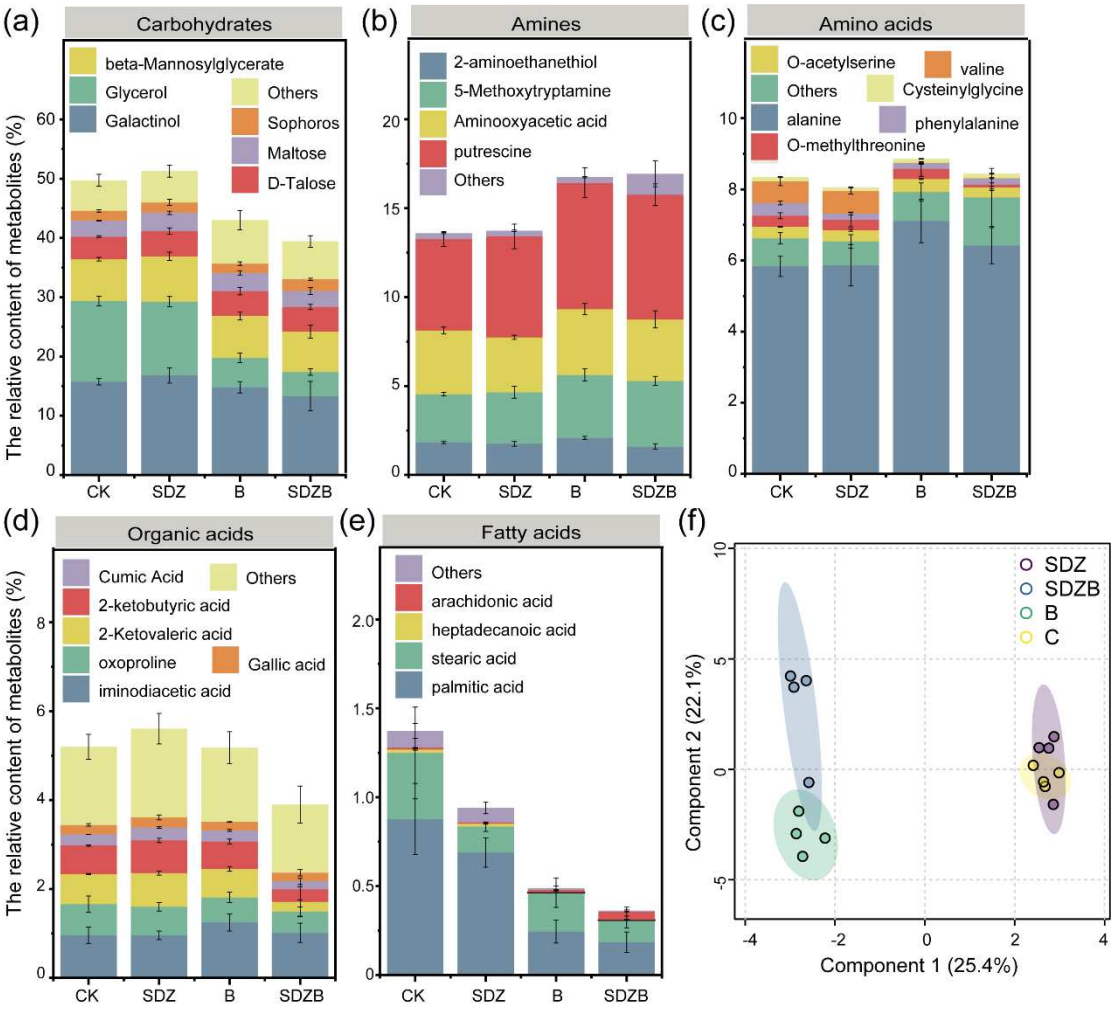
(a)
Carbohydrates
beta-Mannosylglycerate
Glycerol
Galactinol
Others
Sophoros
Maltose
D-Talose
The relative content of metabolites (%)
CK
SDZ
B
SDZB
(b)
Amines
2-aminoethanethiol
5-Methoxytryptamine
Aminooxyacetic acid
putrescine
Others
(c)
Amino acids
O-acetylserine
valine
Others
Cysteinylglycine
alanine
phenylalanine
O-methylthreonine
(d)
Organic acids
Cumic Acid
Others
2-ketobutyric acid
2-Ketovaleric acid
oxoproline
Gallic acid
iminodiacetic acid
(e)
Fatty acids
Others
arachidonic acid
heptadecanoic acid
stearic acid
palmitic acid
(f)
SDZ
SDZB
B
C
Component 2 (22.1%)
Component 1 (25.4%)

Fig. 5

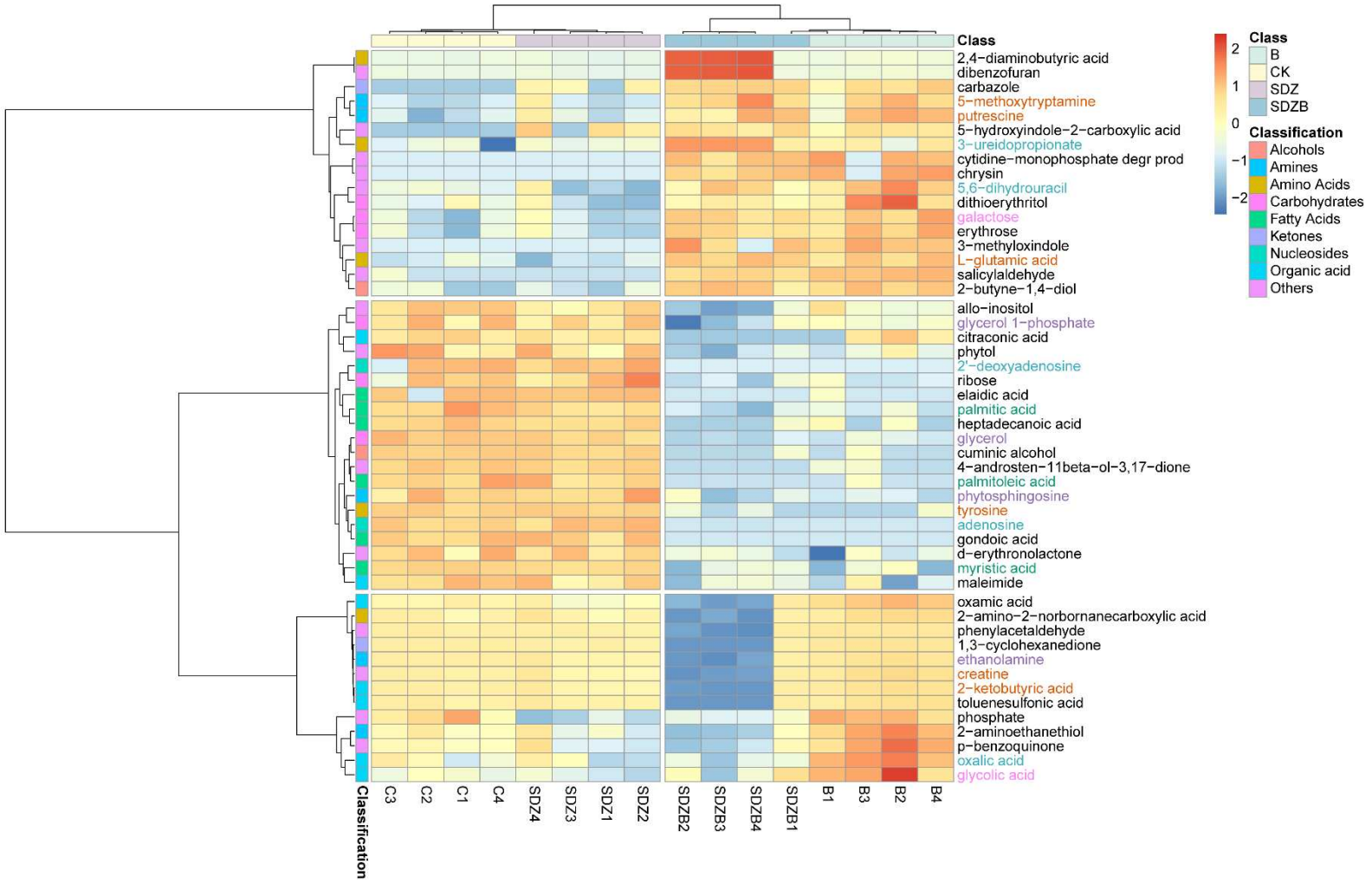
Class
2,4−diaminobutyric acid
dibenzofuran
carbazole
5−methoxytryptamine
putrescine
5−hydroxyindole−2−carboxylic acid
3−ureidopropionate
cytidine−monophosphate degr prod
chrysin
5,6−dihydrouracil
dithioerythritol
galactose
erythrose
3−methyloxindole
L−glutamic acid
salicylaldehyde
2−butyne−1,4−diol
allo−inositol
glycerol 1−phosphate
citraconic acid
phytol
2'−deoxyadenosine
ribose
elaidic acid
palmitic acid
heptadecanoic acid
glycerol
cuminic alcohol
4−androsten−11beta−ol−3,17−dione
palmitoleic acid
phytosphingosine
tyrosine
adenosine
gondoic acid
d−erythronolactone
myristic acid
maleimide
oxamic acid
2−amino−2−norbornanecarboxylic acid
phenylacetaldehyde
1,3−cyclohexanedione
ethanolamine
creatine
2−ketobutyric acid
toluenesulfonic acid
phosphate
2−aminoethanethiol
p−benzoquinone
oxalic acid
glycolic acid
C3
C2
C1
C4
SDZ4
SDZ3
SDZ1
SDZ2
SDZB2
SDZB3
SDZB4
SDZB1
B1
B3
B2
B4
Classification
2
1
0
−1
−2
Class
B
CK
SDZ
SDZB
Classification
Alcohols
Amines
Amino Acids
Carbohydrates
Fatty Acids
Ketones
Nucleosides
Organic acid
Others

Fig. 6

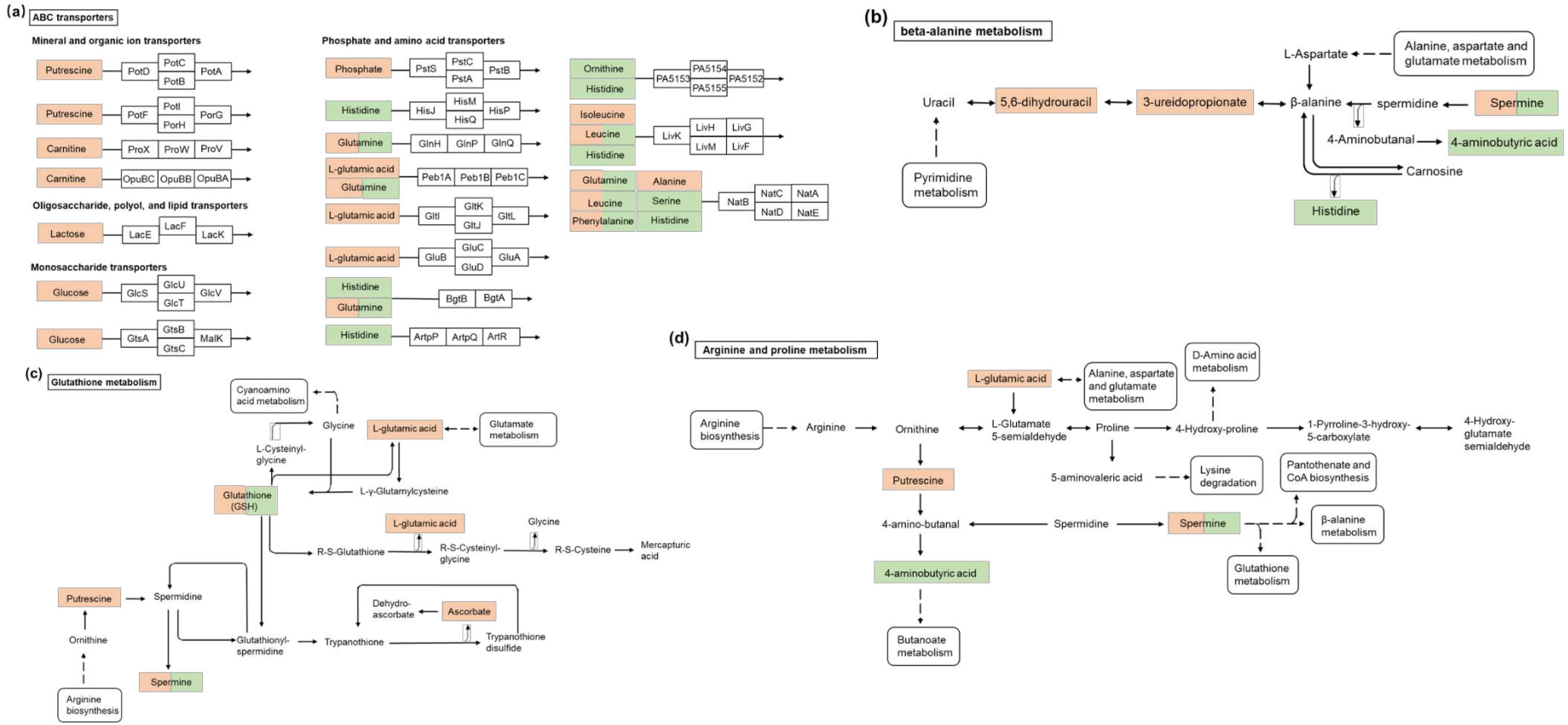
(a)
ABC transporters
Mineral and organic ion transporters
Putrescine
PotD
PotC
PotB
PotA
Putrescine
PotF
PotI
PorH
PorG
Carnitine
ProX
ProW
ProV
Carnitine
OpuBC
OpuBB
OpuBA
Oligosaccharide, polyol, and lipid transporters
Lactose
LacE
LacF
LacK
Monosaccharide transporters
Glucose
GlcS
GlcU
GlcT
GlcV
Glucose
GtsA
GtsB
GtsC
MalK
Phosphate and amino acid transporters
Phosphate
PstS
PstC
PstA
PstB
Histidine
HisJ
HisM
HisQ
HisP
Glutamine
GlnH
GlnP
GlnQ
L-glutamic acid
Glutamine
Peb1A
Peb1B
Peb1C
L-glutamic acid
GltI
GltK
GltJ
GltL
L-glutamic acid
GluB
GluC
GluD
GluA
Histidine
Glutamine
BgtB
BgtA
Histidine
ArtpP
ArtpQ
ArtR
Ornithine
Histidine
PA5154
PA5153
PA5155
PA5152
Isoleucine
Leucine
Histidine
LivK
LivH
LivM
LivG
LivF
Glutamine
Alanine
Leucine
Serine
Phenylalanine
Histidine
NatB
NatC
NatD
NatA
NatE
(b)
beta-alanine metabolism
L-Aspartate
Alanine, aspartate and glutamate metabolism
Uracil
5,6-dihydrouracil
3-ureidopropionate
β-alanine
spermidine
Spermine
4-Aminobutanal
4-aminobutyric acid
Carnosine
Pyrimidine metabolism
Histidine
(c)
Glutathione metabolism
Cyanoamino acid metabolism
Glycine
L-glutamic acid
Glutamate metabolism
L-Cysteinyl-glycine
L-γ-Glutamylcysteine
Glutathione (GSH)
L-glutamic acid
Glycine
R-S-Glutathione
R-S-Cysteinyl-glycine
R-S-Cysteine
Mercapturic acid
Putrescine
Spermidine
Ornithine
Arginine biosynthesis
Glutathionyl-spermidine
Dehydro-ascorbate
Ascorbate
Trypanothione
Trypanothione disulfide
Spermine
(d)
Arginine and proline metabolism
L-glutamic acid
Alanine, aspartate and glutamate metabolism
D-Amino acid metabolism
Arginine biosynthesis
Arginine
Ornithine
L-Glutamate 5-semialdehyde
Proline
4-Hydroxy-proline
1-Pyrroline-3-hydroxy-5-carboxylate
4-Hydroxy-glutamate semialdehyde
Putrescine
5-aminovaleric acid
Lysine degradation
Pantothenate and CoA biosynthesis
4-amino-butanal
Spermidine
Spermine
β-alanine metabolism
4-aminobutyric acid
Glutathione metabolism
Butanoate metabolism

Fig. 7